Structural characterization and photocatalytic activity of electrospun TiO_2 and Ce-doped TiO_2 nanofibers

S. Sang-urai[*], A. Worayingyong[*,**], S. Maensiri[***], M. F. Smith[***,****], S. Seraphin[*****]

[*]Department of Chemistry, Kasetsart University, Bangkok 10900, Thailand,
sarawoot.sang.urai@gmail.com, fsciarw@ku.ac.th
[**]Department of Materials Science, Faculty of Science, Kasetsart University, Bangkok 10900, Thailand
[***]School of Physics, Suranaree University of Technology , Nakhon Ratchasima 30000, Thailand,
santimaensiri@g.sut.ac.th, mfsmith@g.sut.ac.th
[****]Synchrotron Light Research Institute, Nakhon Ratchasima 30000, Thailand
[*****]Department of Materials Engineering, University of Arizona, Tucson, U.S.A,
seraphin@email.arizona.edu

ABSTRACT

Mixed phase TiO_2 and Ce-doped TiO_2 nanofibers with different content (0.5, 2.0, 8.0%) of cerium ions were prepared by a sol-gel electro-spinning method. Results from SEM showed no beads on the undoped-TiO_2 and Ce-doped TiO_2 nanofibers with diameters in the range of 77-130 nm. TEM images exhibited that the undoped TiO_2 crystallite size on the fiber was bigger than those on the Ce-doped samples. XRD and Ti *K*-edge XANES were used to determine anatase/rutile phase ratios in pure TiO_2 nanofibers, whereas only XANES was used to characterize the anatase/rutile phase ratios in the Ce-doped TiO_2 samples. Ce L_3-edge XANES exhibited peak associated with Ce^{+3} (5727 eV.) in addition to Ce^{+4} (5731 and 5738 eV.). Samples with the lowest Ce content had the greatest fraction of Ce ions in the Ce^{+3} state. The photocatalytic activity of the prepared nanofibers was observed by degradation of Rhodamine B under visible light, and the fiber of 0.5 % Ce-doped TiO_2 exhibited the highest activity.

Keywords: titanium dioxide, nanofibers, electrospinning, cerium-doped, XANES

1 INTRODUCTION

TiO_2, one of the promising photocatalysts due to its electrical and optical properties, non-toxicity, stability, can be widely used for elimination of organic pollutant in air and water. It has been prepared in different morphologies such as thin film [1], nanoparticles [2], and nanofiber [3], to enhance its activity under UV-irradiation. Besides, other factors, that effect the photocatalytic activity of TiO_2, are the phase composition [4] and oxygen vacancies [5,6].

To enhance the photocatalytic activity of TiO_2 under visible light, metal dopants can be used. Lanthanide metal, such as Ce being introduced within TiO_2 band gap, makes Ce-doped TiO_2 absorbs photons in the visible region [7,8,9]. The local crystal of TiO_2 nanopariticles and electronic structures of Ce impurities changed with Ce concentration have been reported in the previous work [10]. The spherical TiO_2 nanocrystals showed higher photocatalytic efficiency being subjected to a reduction in the particle size [11,12]. However, in photocatalysis of a practical process, nanoparticles have a tendency to agglomerate into larger particles, thus decreasing the photocatalytic activity. TiO_2 nanofibers, with large aspect ratio, should overcome the disadvantages of using of spherical TiO_2 nanoparticles.

Therefore, this article presents the development of nanostructured Ce-doped TiO_2 in the form of nanofiber to optimize the benefits of Ce-doping in TiO_2. The TiO_2 and Ce-doped TiO_2 nanofibers were prepared by the electrospunning technique and were characterized by XRD, SEM, TEM with SAED and XANES. The photocatalytic activity of the prepared nanofibers was tested by degradation of rhodamine B.

2 EXPERIMENTAL

2.1 TiO_2 and Ce-doped TiO_2 nanofibers preparation

The TiO_2 nanofiber was fabricated by electrospinning a mixture of Ti-prepared sol and polymer. The Ti- sol was prepared by mixing 1.50 g of titanium(IV)isopropoxide (≥97%, Sigma Aldrich) with a mixture of 1.00 g of ethanol and 3.00 g of glacial acetic acid (99.9%, Merck). The mixture precursor with poly(vinylpyrrolidone):PVP was stirred for 6 h at room temperature to attain sufficient viscosity for electrospinning. The mixture solution was fed at a rate of 1 cm^3/h using a syringe pump. Nanofiber samples were collected on an aluminum foil collector [13,14]. The electrospun PVP/TiO_2 composite was dried at 333 K for 12 h. and then calcined at 823 K with a heating rate of 1.7 K/min for 4 h. The obtained sample would be referred to the undoped TiO_2 nanofiber.

In case of Ce-doped TiO_2 nanofibers, 0.5, or 2.0 or 8.0 %Ce (with respect to Ti weight) of ceriumacetylacetonate (Aldrich) was added into the Ti-prepared sol, and followed the same method as that descrilbed above. The prepared nanofibers were denoted as $0.5Ce/TiO_2$, $2Ce/TiO_2$, and $8Ce/TiO_2$ respectively.

2.2 Characterization

TiO_2 nanofibers were characterized morphologically by scanning electron microscope (SEM, Hitachi S-3400N) and transmission electron microscope (TEM, 200kV FEI Tecnai G2 20 Super-Twin); their phase constitution were investigated by X-ray diffraction (XRD, Bruker D8 ADVANCE Powder XRD); XAS measurements were performed in transmission mode at the X-ray absorption spectroscopy beamline (BL7.3 and BL8) of the Synchrotron Light Research Institute, Thailand. To prepare the samples for measurements in a transmission mode, each TiO_2 sample was deposited on Kapton tape. The photon energy was calibrated by measuring the absorption edge of Ti foil and compare with the literature.

X-ray absorption spectra at the Ti *K*-edge are measured in transmission mode using Ge (220) double-crystal monochromator. The data accumulation times were 2, 0.5, 0.05K sec/0.2 energy step. The operating pressure of ionization chamber (I_0) was 15 mbar of argon in helium. The sample chamber was in inert atmosphere. The Ti foil was used to calibrate the *K*-edge absorption peak at 4966 eV. The EXAFS spectra measurement was in photon energy range of 4866 – 5611 eV.

X-ray absorption spectra at the Ce L_3-edge were measured in fluoresence mode using Ge(220) double-crystal monochromator. The data accumulation times were 0.3 sec/step for XANES and 2, 0.5, 0.05 Ksec/step for EXAFS. The operating pressure of ionization chamber (I_0) was 15 mbar of argon in helium. The sample chamber was in inert atmosphere. The CeO_4 is used to calibrate the L_3-edge absorption peak at 5731 eV. The XANES spectra measurement was in photon energy range of 4895–5085 eV.

2.3 Photocatalytic experiment

The photocatalytic activity of the prepared TiO_2 nanofiber was observed by the degradation of a standard solution of rhodamine B (RhB) in a photochemical reactor under visible light irradiation. A total of 50 mg of each catalyst was added into 50 mL of the above $2x10^{-5}$ M of rhodamine B (RhB) solution in a quartz cell. Before irradiation, the suspensions were dispersed in ultrasonic bath for 30 min and magnetically stirred in dark for 30 min to ensure the establishment of an adsorption/desorption equilibrium. The above suspensions were kept under constant air-equilibrated conditions before and during the irradiation. At given time intervals, about 4 mL of suspensions were sampled and centrifuged at 5000 rpm to remove the catalyst. The filtrates were analysed by measuring the maximum absorbance of rhodamine B (RhB) at 566 nm under the same experimental conditions.

3 RESULTS AND DISCUSSION

HRTEM images of the calcined TiO_2 and Ce-doped TiO_2 nanofibers indicated that each fiber was formed through the sintering of TiO_2 nanoparticles (Fig. 1a-b). The undoped TiO_2 nanofiber composed of particles with diameters ranging from 15-30 nm (Fig. 1(a)), whereas particle sizes of Ce-doped TiO_2 nanofibers were decreased to less than 15 nm in diameters (Fig. 1(b)).

The inset in the SAED patterns of the undoped TiO_2 nanofiber in Fig. 1a showed the (101) plane of anatase and the (110) plane of rutile indicating the mixture phases of anatase and rutile in the TiO_2 crystalline on the nanofiber.

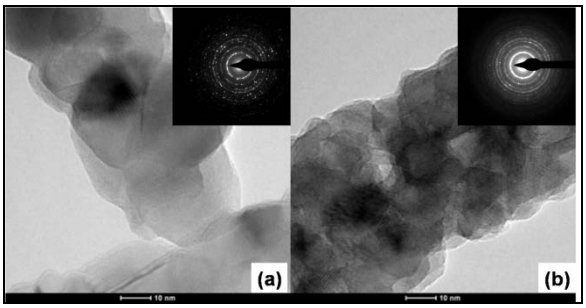

Figure. 1: HR-TEM of (a) TiO_2 nanofibers and (b) $8Ce/TiO_2$ nanofibers

The SAED patterns of the Ce-doped TiO_2 crystal (Fig. 1b) showed only the anatase phase and the crystal size of TiO_2 reduced with increasing the cerium concentration. The effect of Ce blocked TiO_2 crystal formation in the nanofiber corresponded to that reported in literature [15].

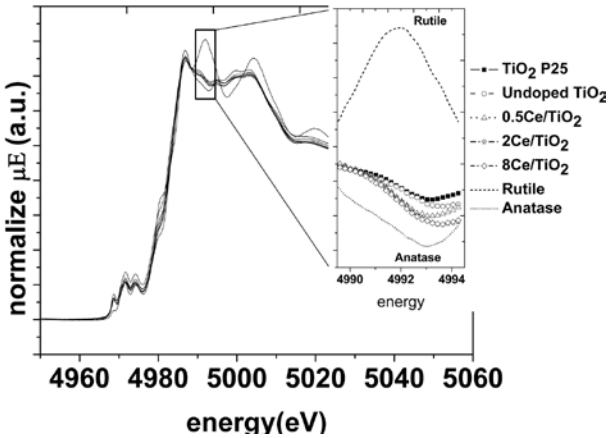

Figure. 2: Ti *K*-edge XANES spectra of TiO_2 and Ce-doped TiO_2 nanofibers

XANES spectra of TiO_2, Ce-doped TiO_2 nanofibers TiO_2-P25, the anatase and rutile TiO_2 showed different

features (Fig. 2). The average weight fractions of anatase and rutile in all nanofiber samples were calculated by comparison with the XANES spectra of the anatase and rutile standards as exhibited in the inset of the XANES spectra of all nanofibers. The results are presented in Table 1. The anatase percentage of TiO_2-P25 determined from XANES compared with that from XRD confirmed that the methods could be applied for the anatase percentage determination of all nanofibers. It can be noticed that the undoped TiO_2 nanofiber has the anatase percentage almost the same value of TiO_2-P25.

samples	% anatase		Crystal size
	(XRD)	(XANES)	(nm)
TiO_2-P25	71.7	73.7	34
Undoped TiO_2	79.2	75.6	24
0.5Ce/TiO_2	-	79	19
2Ce/TiO_2	-	81.1	17
8Ce/TiO_2	-	82.3	15

Table 1: The calculated anatase percentage of TiO_2 and Ce/TiO_2 nanofibers from XANES spectra compared with the rutile and anatase standard

The results of the anatase percentages from the Ce-doped TiO_2 nanofibers indicated that the anatase phases increased when increasing cerium concentration, which confirmed that Ce blocked the rutile formation [15].

Ce L_3-edge fluorescence XANES spectra of the local structures of Ce ions in 0.5Ce/TiO_2, 2Ce/TiO_2 and 8Ce/TiO_2 nanofibers are shown in Fig 3. From Ce L_3-edge XANES, Ce^{+3} of ceriumacetylacetonate exhibited the white line at 5726 eV (B_0) and Ce^{+4} of CeO_2 standard has two absorption peaks at 5731 (B_1) and 5737 (C) eV. The transitions of B_0, B_1 and C were explained in reference[10]. B_0 is denoted as the transition of electrons in Ce^{+3} from Ce core $2p^{3/2}$ state upto $4f^1$ (for which the state $|4f^1>$ is not associated with a ligand hole). Peaks B_1 and C are denoted as the transitions of Ce^{+4}, of which the initial state is described as two states [16]. B_1 is a strong transition from the ground state to the $|4f^1>$ configuration and peak C is a strong transition from the ground state to the $|4f^0>$ final state. The samples 2Ce/TiO_2 and 8Ce/TiO_2 nanofibers exhibited absorption peaks at B_1 and C, which corresponded to the transitions of electrons in Ce^{+4} state, and small shoulder at B_0, indicating small fraction of Ce^{+3} state in these samples. The strength of B_1 compared to C is related to the ground state weights, which determine the extent of Ce ions formally Ce^{+4} borrowing electrons from ligand neighbors. If Ce 4f states become strongly hybridized with ligand orbitals then the electron hopping frequencies increase, and B_1 grows relative to C [10]. The 2Ce/TiO_2 nanofiber exhibited the absorption peak at B_1 being stronger than that at C,showing that the Ce^{+4} state in this sample is strongly hybridized with ligand orbitals. To compare with the B_1 intensity of 8Ce/TiO_2, it can be concluded that the Ce^{+4} state in 8Ce/TiO_2 is hybridized with ligand orbitals less than that of 2Ce/TiO_2. Whereas 0.5Ce/TiO_2 nanofiber exhibited very intense absorption at B_0 indicating the presence of the Ce^{+3} state. All samples had the transition from the ground state to the $|4f^0>$ final state at peak C indicating the presence of the Ce^{+4} state, with decreasing amount upon the reduced Ce contents. It has been reported that the high Ce content sample has the Ce in the substitution of Ti position as observed by EXAFS [17], corresponded to the preferred state of Ce^{+4}. With high Ce concentration, the crystal structure in TiO_2 is being distorted as a result, the 4f orbitals of the Ce atoms are less hybridized with the p-orbitals of the oxygen neighbors, corresponded to those of Ce doped TiO_2 nanoparticles in the previous work[10].

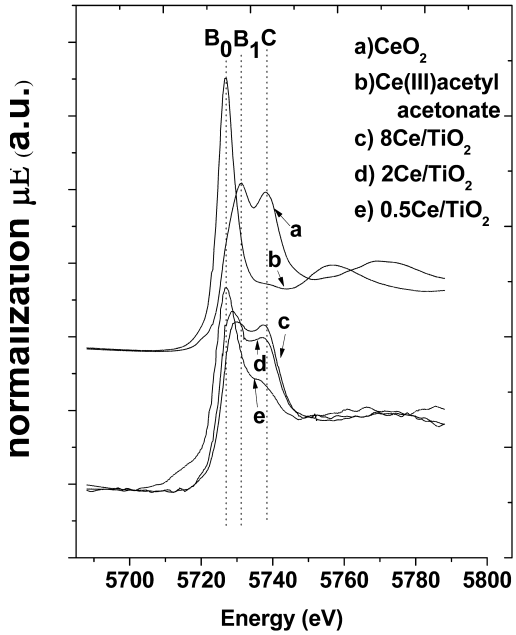

Figure. 3: Ce L_3-edge XANES fluoresence spectrum of (a) CeO_2 (b) Ce(III)acetylacetonate (c) 8Ce/TiO_2 nanofibers (d) 2Ce/TiO_2 nanofibers (e) 0.5Ce/TiO_2 nanofibers

The low Ce content (0.5%), showing mainly the Ce^{+3} state and a small indication of Ce^{+4} as a shoulder of peak C (less hybridization with the oxygen neighbor), could be assumed that the Ce ion in the TiO_2 nanofiber is in an interstitial position.

The absorption spectra of all prepared nanofibers in the region of 200-600 nm were observed but the spectra were not shown here. The Ce-doped TiO_2 nanofibers exhibited absorption around 400-450 nm., and the intensities increased when the Ce contents were higher. The lowest Ce content; 0.5Ce/TiO_2 nanofiber, absorbed the visible light at 400 nm a little bit higher in intensity than the undoped one. The red-shift of the Ce-doped TiO_2 nanofibers could be attributed to transitions in two cases, which are adapted from that described in literature [18] as follows: 1) an excitation from the valence band of TiO_2 to Ce 4f level, and 2) an excitation from the ground state of Ce species to Ce 4f level. In the case of 0.5Ce/TiO_2 nanofiber, the Ce species is

mainly Ce^{+3} with small amount, the absorption could be attributed mainly to Case 1, which has Ce^{+3} ion lower the band gap energy of TiO_2 into the visible region. For the high Ce contents ($2Ce/TiO_2$ and $8Ce/TiO_2$ nanofibers), the absorptions in the visible region could be attributed to Case 2, which refers to the excitation of the Ce species being mainly Ce^{+4} to Ce 4f level. Therefore, it could be assumed that the photocatalysis mechanism of the low Ce content is different from that of the high Ce content.

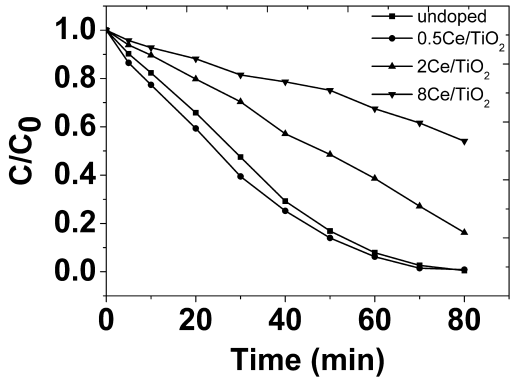

Figure 4: Photocatalytic activity of TiO_2 and Ce/TiO_2 nanofibers determine by photocatalytic degradation of RhB under visible-light irradiation

The photocatalytic activities of TiO_2 and Ce-doped TiO_2 nanofibers were tested by the degradation of rhodamine B (RhB) in aqueous solution under visible light irradiation (Fig 4) and the $0.5Ce/TiO_2$ nanofibers exhibited the high activities with the completion of RhB degradation in 80 min. With small amount of Ce, the fiber absorbs visible light better that the undoped TiO_2, produces more photo-electrons for the degradation. But the activities decreased dramatically when the Ce content was higher. The mechanism of the photocatalytic oxidation is adapted from that described in literature [19]. The photocatalysis of the nanofiber with low Ce-concentration could be explained such that: Cerium ion is more likely with +3 valences and forms oxygen vacancies, which can activate oxygen molecules becomming active oxygen species for oxidation of RhB. Secondly, Ce^{+4} which exists as some fraction in the fiber can trap the photo-excited electron and the hole carriers can move to the sample surface to activate a hydroxide ion forming a hydroxyl radical available for the oxidation of RhB. Together with the Ce effect, the $0.5\%Ce\text{-}TiO_2$ sample has the anatase/rutile phase ratio of 79/21(almost equivalent to TiO_2-P25), which could separate holes from electrons to the fiber surface via the valence band lined up between the two phases [4]. Thus the photocatalytic activity of the $0.5\%Ce/TiO_2$ nanofiber should be due to the active surface oxygen species upon the Ce^{+3} species and the electron/hole separation upon the valence band energy lined up of the rutile and anatase phases. When the Ce-concentration was higher, the activities were lower. It confirms that the Ce^{+4} site temporarily trapped an electron, which later can escape and might recombine with the active hole and then reduced the photocatalytic activity.

4 CONCLUSIONS

The TiO_2 and Ce-doped TiO2 with 0.5, 2.0, 8.0 % of cerium ions nanofiber catalysts were successfully prepared by the sol-gel electrospinning method using poly(vinylpyrrolidone) polymer as binder. The catalysts of Ce-dopants affected the ratio of anatase to rutile and the crystal sizes of TiO_2 in the nanofibers. Ti *K*-edge XANES indicated that the anatase percentage of the undoped TiO_2 nanofiber was almost the same value of TiO_2-P25 and increased with increasing the cerium contents. Ce L_3-edge XANES of the lowest Ce content TiO_2 nanofibers showed the greatest fraction of Ce ions in the Ce^{+3} state, which resulted in the highest activity of Rhodamine B degradation under visible light irradiation.

REFERENCES

[1] S. Kityakarn, Y. Pooarporn, P. Songsiriritthigul, A. Worayingyong, S. Robl, A. M. Braun, and M. Worner, Electrochim. Acta. 83, 113, 2012.
[2] L. Dan and X. Younan, Nano Lett. 3, 6. 2003
[3] A. R. Rao, and V. Dutta. Sol. Energ. Mat. Sol. C. 91, 1075, 2007.
[4] Y. Pooarporn, Ph.D. dissertation, Chemistry Dept., Kasetsart Univ., Bangkok, Thailand, 2008.
[5] R. Schaub, et al.,. Science. 299, 377, 2002.
[6] I. Nakamura, N. Negishi, S. Kutsuna, T. Ihara, S. Sugiha and K. Takenchi. J. Mol Catal. A: Chem. 161, 205, 2000.
[7] A. Silva, C. Silva, G. Drazic, J. L. Faria Catal. Tod. 144, 13, 2009.
[8] J. Fang, et al.. Appl. Surf. Sci. 253, 8952, 2007.
[9] X. Bokhimi and R. Zanella, J. Phys. Chem. C. 111, 2525, 2007.
[10] S. Kityakarn, A. Worayingyong, A. Suramitr, M. F. Smith. Mater.l Chem. Phys. http://dx.doi.org/10.1016/j.matchemphys.2013.01.055
[11] A. R. Rao, and V. Dutta, Sol. Energ. Mat. Sol. C. 91, 1075, 2007.
[12] K. Porkodi and S.D. Arokiamary. Mater. Charac,. 58. 495, 2007.
[13] H. Li, et al., J. Am. Chem. Soc. 93, 2503, 2010.
[14] H. Li, W. Zhang, and W. Pan, J. Am. Chem. Soc, 94, 3184, 2011.
[15] C. Zhao, et al., Catal. Sci. Technol. 2, 2558, 2012.
[16] S.H. Overbury, D. R. Huntley, D.R. Mullins and G. Vlaic, J. Sych. Rad. 6, 34, 1998.
[17] A. Niltharach, Ph.D. dissertation, Chemistry Dept., Kasetsart Univ., Bangkok, Thailand, 2011.
[18] J. Xiea, et al., Colloids Surf., A. 372, 107, 2010.
[19] Z. Liu, B. Guo, L. Hong, H. Jiang, J. Phys. Chem. Solids. 66, 161, 2005.